DOI 10.4430/bgo00416

Towards a crustal structure investigation in the area of Mefite d'Ansanto (Italy) by using equalised teleseismic waveforms

G. Milano[1], S. Morabito[1], A. Gervasi[2] and P. Cusano[1]

[1] *Istituto Nazionale di Geofisica e Vulcanologia, Sezione di Napoli - Osservatorio Vesuviano, Naples, Italy*
[2] *Istituto Nazionale di Geofisica e Vulcanologia, Osservatorio Nazionale Terremoti, c/o UniCal, Rende (CS), Italy*

(Received: 15 December 2022; accepted: 27 February 2023; published online: 28 April 2023)

ABSTRACT We propose and test a procedure in the time domain to directly compare the waveforms of teleseismic events recorded by seismic stations located a few kilometres from each other and equipped with different instrumentations. The method is based on the deconvolution of the signals at each seismic station for its sensor own frequency response and data sampling to equalise the waveforms, making them directly comparable. The horizontal components of the events are rotated versus back-azimuth, considering that P-to-S converted phases along a crustal discontinuity are generally more evident in the radial and transverse components. Finally, we apply the cross-correlation technique to the resulting signals to quantify the similarities among the waveforms. The method has been tested on teleseismic events recorded by the seismic stations located in and close to the Mefite d'Ansanto area (southern Apennines), which represents the largest non-volcanic low temperature CO_2 emission area on Earth.

Key words: equalisation procedure, cross-correlation, teleseismic events, Mefite d'Ansanto, crustal structure, southern Apennines.

1. Introduction

Mefite d'Ansanto is the largest non-volcanic low temperature CO_2 emission area on Earth (Chiodini *et al*., 2010). The site is located in the central part of the southern Apennines, between the Sannio and Irpinia seismogenic regions (Fig. 1). FURTHER, "The role of FlUids in the pReparaTory pHase of EaRthquakes in southern Apennines", is an INGV (*Istituto Nazionale di Geofisica e Vulcanologia:* National Institute of Geophysics and Volcanology) Department Strategic Project whose purpose is to outline how fluids are involved in the generation of earthquakes in specific areas, among which Mefite d'Ansanto (Fig. 1) is one of the most interesting. At this site, several instrumentations have been installed in the area surrounding both the CO_2 emission vents and the channel where the gas flows, so as to carry out a multidisciplinary survey aimed at monitoring fluid dynamics (https://progetti.ingv.it/en/further; last access: November 2022). In this framework, efforts are addressed to the development and application of methodologies to investigate the crustal structure beneath the Mefite d'Ansanto area.

In the last decades, several studies have been carried out to delineate the crustal structure of the southern Apennines that comprises the Mefite d'Ansanto area. Amato *et al*. (1992) inferred

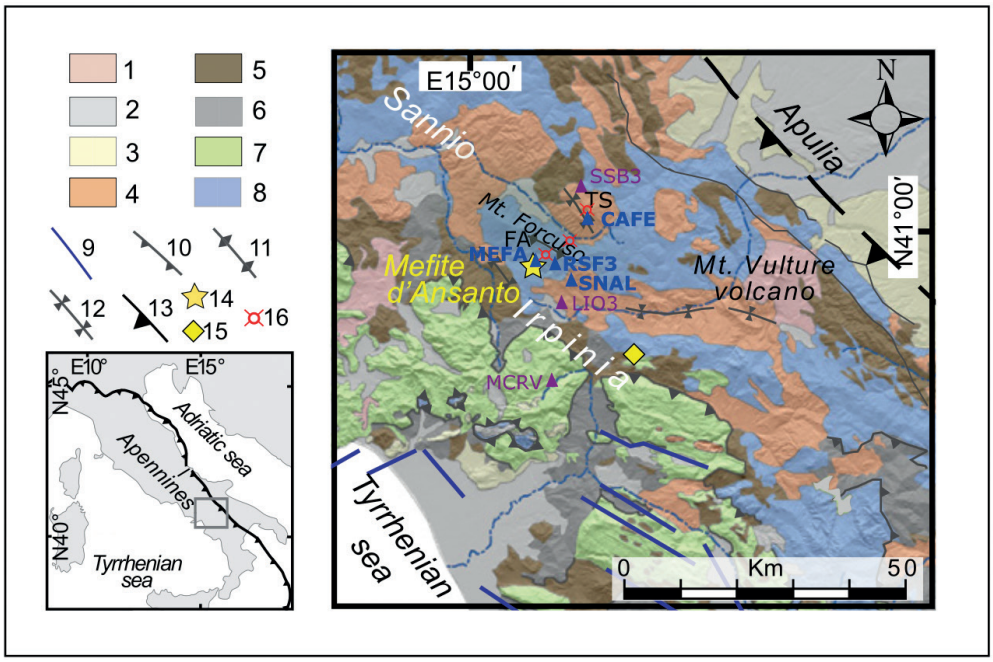

Fig. 1 - Geological map of the Irpinia region along the southern Apennines, with location of Mefite d'Ansanto (modified after Ascione *et al.*, 2018): 1 = Middle Pleistocene to Holocene volcanics; 2 = lower Middle Pleistocene to Present deposits; 3 = Lower Pleistocene to lower Middle Pleistocene wedge-top and foreland basin deposits; 4 = late Lower Pliocene to Lower Pleistocene wedge-top and foreland basin deposits; 5 = Miocene wedge-top and foreland basin deposits; 6 = Basinal succession (Mesozoic-Tertiary); 7 = Apennine platform carbonates (Mesozoic-Tertiary); 8 = Lagonegro - Molise deposits (Mesozoic-Tertiary); 9 = main faults; 10 = main thrust faults; 11 = axis of main antiforms; 12 = axis of main synforms; 13 = buried thrust front; 14 = non-volcanic gas emission; 15 = 1980 earthquake epicentre location; FA = Frigento antiform, TS = Trevico synform (after Pischiutta *et al.*, 2013); 16 = position of the stratigraphic wells [from south to north: Mt. Forcuso 1, Mt. Forcuso 2, and Trevico 1 wells (ViDEPI, 2016)]. Seven of the seismic stations employed in the Irpinia region during 2021 are indicated as triangles. The four seismic stations used in this study are in blue.

the velocity structure underneath a large area centred at the epicentre of the 23 November 1980, M_s (surface-wave magnitude) = 6.9, earthquake, using the traveltimes relative to the earthquakes recorded by a local network. Those authors found a sharp P-wave velocity contrast at a depth of about 10 km, along which the main rupture occurred. Chiarabba and Amato (1997), modelling the direct and refracted P-wave traveltimes in the Benevento region at the northern edge of the Irpinia fault using P-wave earthquake arrival times from 1991 to 1992, found strong heterogeneities in the first 6 km of crust. These heterogeneities were likely related to the high velocity carbonate platform units thrusting towards the NE. The authors also detected high velocities at a 9 km depth that were related to an up-thrust of lower-crust rocks. Improta *et al.* (2003) investigated the upper crustal structure of the Irpinia region through the analysis and interpretation of gravity data, seismic reflection lines, and borehole stratigraphies. These authors found significant lateral density variations likely linked to NW trending geological structures and highlighted the abrupt Apulia Carbonate platform deepening towards the south-eastern edge of the investigated area. In the epicentral region of the 1980 event, they found a good correlation between the high density and high velocity of the Apulia platform carbonates. Despite the above studies, no detailed information on the crustal structure beneath the Mefite d'Ansanto area is available.

The analysis of teleseismic events can provide information about the depth and dip of the main crustal discontinuities beneath an extended area around the recording seismic station. This analysis is based on the identification of P-to-S and S-to-P converted phases generated by the interaction of an incident P or S wave with velocity discontinuities beneath the receiving station (Clayton and Wiggins, 1976; Langston, 1979; Ammon, 1991). This approach considers the modelling of the crustal structure beneath the observation point using synthetic seismograms for P and SV waves and implies the comparison between synthetic and observed data to obtain the best fit. Such method can be applied to deep or intermediate earthquakes, since the incident time function of teleseismic events can often be modelled as a single unidirectional pulse. A different approach is applied if data of deep or intermediate events are not available. In these cases, the observed data are equalised to compensate for different source time functions by applying the Receiver Functions technique (Langston, 1979). After removing source and path-effects, this technique enables identifying converted and reverberated phases in the crust generated by the interaction of a teleseismic P wave with a discontinuity surface in the crust. The technique is based on the assumption that the vertical component of a teleseismic event contains undesired source and path effects and is not significantly contaminated by the near receiver structure. A fundamental step towards the application of the above methodologies requires direct comparison between the records of the different seismic stations, whose instrumental responses are known, arranged along suitable profiles.

The analysis of teleseismic events to investigate the crustal structure of an area has also been applied to seismic signals recorded by seismic stations belonging to a permanent monitoring seismic network and equipped with short-period seismometers (Milano *et al*., 2001). In this case, information can also be obtained both on deep discontinuities (e.g. Moho) and on subsurface discontinuities (< 5 km) if the instrumental response of the used instrumentation is known. When instruments with different characteristics are used, e.g. dissimilar datalogger and sensors, it is necessary to make the recorded data comparable.

Here, we propose and test a procedure, in the time domain, to directly compare the waveforms of teleseismic events recorded by the seismic stations located a few kilometres from each other and equipped with different instrumentations. The procedure we propose is targeted to make the recorded data comparable and is based on the application of the waveform cross-correlation technique. To make the signals comparable, the seismograms are corrected for the instrumental response, resampled and filtered. The thus processed signals are termed 'equalised' in the following. The ultimate goal is the investigation of the upper crustal structure, beneath the Mefite d'Ansanto and surrounding areas, to obtain information on how large and deep the area of diffuse CO_2 degassing is. The test has been performed using selected teleseismic events recorded by the seismic station (MEFA), installed close to the Mefite d'Ansanto main emission vents in the framework of the FURTHER project, by the permanent seismic stations of the National Seismic Network (IV) and the Irpinia Seismic Network (IX) located at less than 10 km from the emission vents (Fig. 1).

2. Tectonic overview of the area

Mefite of the Valle d'Ansanto (Fig. 1) is located in the southern Apennines fold and thrust belt, part of the Alpine-Apennine orogenic system, that evolved within the overall framework of the Africa-Europe major plate convergence since the Late Cretaceous (e.g. Mazzoli and Helman, 1994). The southern Apennines accretionary wedge includes several superposed tectonic units derived from both ocean and continental margin domains (e.g. Mostardini and Merlini, 1986; Patacca

and Scandone, 1989). The continental margin-derived units (Apennine Platform and Lagonegro - Molise Basin successions) are stratigraphically overlain by Neogene foredeep and wedge-top basin sediments (e.g. Mazzoli *et al*., 2012). The Apennine accretionary wedge is thrusted onto the Apulian platform, which has a thickness of 6–8 km and represents the buried part of the succession exposed in the foreland to the NE (e.g. Mostardini and Merlini, 1986; Shiner *et al*., 2004). The buried Apulian Platform is affected by reverse-fault-related, long-wavelength folds that form the hydrocarbon traps for the most important oil fields in southern Italy (Shiner *et al*., 2004). Evidence is also given of the local occurrence of CO_2 gas caps in the top part of structural culminations made of fractured Apulian Platform carbonates (e.g. Improta *et al*., 2014).

The central-axial part of the southern Apennines, where the study area is set, is characterised by an extreme structural complexity of the thrust belt, as highlighted by a great deal of seismic reflection and well data coming from hydrocarbon exploration (Mostardini and Merlini, 1986; Patacca and Scandone, 1989; Roure *et al*., 1991). The Mefite degassing area lies on the western flank of the structural high of the Frigento Antiform, which hosts Mt. Forcuso, and where calcareous-siliciclastic and marly deposits of the Lagonegro units crop out (Matano and Di Nocera, 2001; ISPRA, 2016). At depth, well and seismic profile data show that Miocene siliciclastic deposits of the Lagonegro units tectonically cover the Cretaceous Apulian Platform carbonates (Mostardini and Merlini, 1986; Improta *et al*., 2003; ViDEPI, 2016) that can be found at shallow depth (top at 1128 m of depth, Mt. Forcuso 1 well, Fig. 1).

A large part of the background seismicity roughly aligns along the chain axis, as well as the distribution of events that produced historical earthquakes (e.g. Castello *et al*., 2008; Frepoli *et al*., 2011; Di Luccio *et al*., 2022). Earthquakes with magnitude larger than 6.5 occur along NW-SE striking faults (Di Luccio *et al*., 2022) related to the active extensional regime. Nevertheless, a moderate (moment magnitude, $M_w \leq 5.5$) deep-seated seismicity (> 18 km of depth) linked to strike-slip kinematics in the intermediate/deep crust is also present at the border between the Irpinia and Sannio regions, thus suggesting the co-existence of different tectonic styles at different crustal depths (De Matteo *et al*., 2018).

The Valle d'Ansanto lies between the Sannio and Irpinia seismogenic regions that are considered among the most active seismic areas of Italy. These regions are affected by different fault systems, some of which likely have a seismogenic role (DISS Working Group, 2021). Several historical destructive earthquakes struck these regions [e.g. M_w = 7.06, 1688 Sannio, and M_w = 6.75, 1732 Irpinia; Rovida *et al*. (2020, 2022)]. Among the most recent and strongest, the M_S = 6.9, 1980 Irpinia earthquake caused ca. 3,000 causalities and produced, in the epicentral area, a large number of significant geological effects, such as ground deformations, landslides, liquefactions, and variations of spring discharge rates (Ascione *et al*., 2020).

In these regions, a link between earthquake occurrence and presence of fluids has been evidenced in some papers (e.g. Chiodini *et al*., 2010; Amoroso *et al*., 2017). In the Mefite area, the gas leakage is probably linked to the presence of active fault systems that are responsible for the large historical earthquakes in the region (Chiodini *et al.*, 2010; Pischiutta *et al.*, 2013).

3. Data and methods

We utilised the data recorded by MEFA (Table 1), a stand-alone seismic station installed about 100 m north of the main Mefite emission vents (Cusano *et al*., 2021; Morabito *et al.*, 2023). This station was installed on 20 November 2020 and the signals were telemetered via UMTS to the server in Naples (INGV). The station recorded continuous signals until 31 March 2021. Moreover,

we used the data recorded by some permanent seismic stations of the national and Irpinia seismic networks. As shown in Fig. 1, at least six stations employed in the Irpinia region in 2021, together with the MEFA station, are roughly aligned along N-S (Milano *et al.*, 2022). Among these, here we used the stations indicated with blue triangles in Fig. 1 and listed in Table 1.

Table 1 - Seismic station information. AV indicates the Avellino province.

Station name and locality	Network	Latitude N (°)	Longitude E (°)	Elevation (m)	Sensor datalogger	Sps (Hz)
CAFE Carife (AV)	INGV (IV)	41.0280	15.2366	1070	Nanometrics Trillium-40s Nanometrics Trident	100
MEFA Mefite (AV)	FURTHER	40.9756	15.1461	710	Guralp CMG40T-60s Lunitek Atlas	100
RFS3 Rocca San Felice (AV)	IRPINIA (IX)	40.9643	15.1760	865	Nanometrics Trillium-40s Agecodagis Osiris	125
SNAL Sant'Angelo dei Lombardi (AV)	INGV (IV)	40.9254	15.2091	874	Nanometrics Trillium-40s Nanometrics Trident	100

We selected the teleseismic events related to deep and intermediate earthquakes with an epicentral distance $\Delta \leq 95°$, $M \geq 6.0$ and recorded by the selected stations. After a visual inspection of the seismograms, we chose the events showing impulsive onsets (see examples in Figs. 2 and 3) since the incident time function of such events can often be modelled as a single unidirectional pulse. The chosen seismic stations are equipped with broadband sensors having

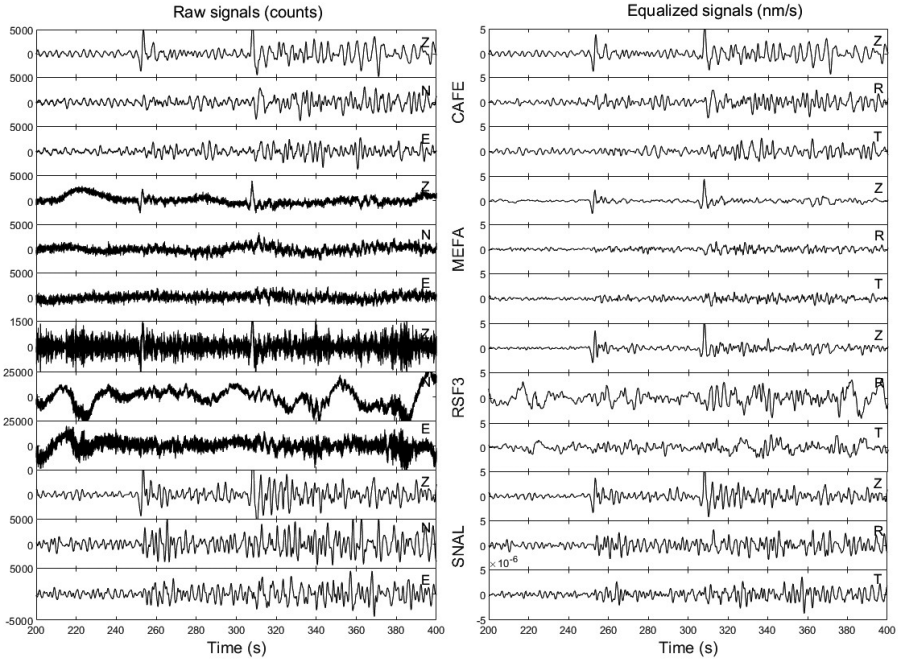

Fig. 2 - Seismograms of the first 150 s of the teleseismic event of 8 January 2021 (Table 2). Left side: raw signals recorded by the three-component stations CAFE, MEFA, RSF3 and SNAL. Right side: equalised signals.

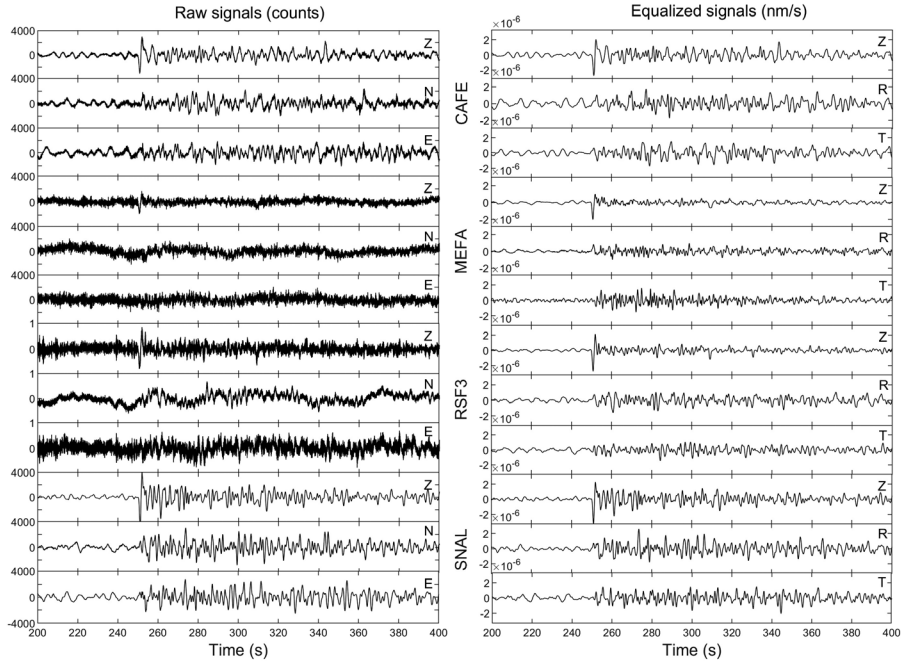

Fig. 3 - Seismograms of the first 150 s of the teleseism of 26 March, 2021 (Table 2). Left side: raw signals recorded by the three-component stations CAFE, MEFA, RSF3 and SNAL. Right side: equalised signals.

different frequency response and the data are acquired with different sampling rates (see Table 1). The direct comparison between the waveforms recorded at the selected seismic stations to evaluate the presence, if any, of converted phases on the same subsurface discontinuity, could not be carried out correctly. To make our data set homogeneous, we proceeded as follows. The signals of each station were deconvolved for their own sensor frequency response and the sampling rate was uniformed to 100 Hz. In detail, RSF3 signals were first up-sampled (factor of 4) and then down-sampled (factor of 5) to pass from 125 to 100 Hz. Successively, the horizontal components of each event were rotated versus back-azimuth to obtain the radial and transverse components. This process is required because P-to-S converted phases are generally more evident on the radial and transverse components of a seismogram. Finally, we applied a zero-phase-shift, 2 Hz low-pass filter to exclude undesired high frequency noise. Figs. 2 and 3 show two examples of teleseismic events as recorded at the selected stations (raw signals, on the left) and the corresponding equalised tracks (on the right). In these two figures the seismograms are ordered from north to south (see Fig. 1).

In Table 2 the parameters relative to the teleseismic events used in this paper are reported. The listed traces were extracted from the FURTHER archive for the MEFA station and EIDA database (INGV, available at https://eida.ingv.it/it/; last access: December 2022) for the other stations.

Table 2 - List of the teleseismic event parameters used in this study.

Date (yyyymmdd)	Origin time (hh:MM:ss)	Lat N (°)	Lon E (°)	Depth (km)	MW	Δ (°)	Baz (°)	Zone
20210108	00:28:49	29.59	-178.66	220	6.1	64.5	46.7	Kermadec Islands, New Zealand
20210112	02:39:42	43.75	140.05	200	5.9	82.6	36.3	Hokkaido, Japan
20210326	22:02:16	26.11	125.0	157	5.9	90.3	60.1	NE of Taiwan

The waveform cross-correlation technique is an efficient tool used in the detection and characterisation of seismic signals since their processing often requires the measurement of the similarity or the time alignment of the traces. As a measure of the similarity between two waveforms, the cross-correlation technique is widely applied in various stages of data processing: detection of low magnitude seismic events (Gibbons and Ringdal, 2006; Harris and Paik, 2006; Schaff and Waldhauser, 2006), location of seismic events (Schaff and Waldhauser, 2005; Schaff and Richards, 2011), phase identification and characterisation (Harris and Dodge, 2011), and event clustering (Harris and Dodge, 2011). To quantify the similarities among the waveforms of the teleseismic events recorded by the selected seismic stations, we applied the cross-correlation technique to the equalised signals, after band filtering in 0.05-2.0 Hz. The filtering is necessary to reduce local seismic noise.

4. Results and discussion

Since we are interested in investigating the crustal structure beneath a broad area around the Mefite d'Ansanto emissions, we took the MEFA station as reference and calculated the cross-correlation function between this station and the other three, component by component, for each of the earthquakes listed in Table 2. The results for the teleseismic events of 8 January are shown in Fig. 4, and of 26 March in Fig. 5, while the results for the event of 12 January are only mentioned in the text (see below). The cross-correlation function was applied over time windows of 20 s, centred in correspondence of the first P-wave arrivals at each station, with about 10 s of pre-event background noise (see left side of Figs. 4 and 5).

The vertical components show high maximum values of the correlation function, always above 0.7 (see the right side of Figs. 4a and 5a). Moreover, they display a systematic spatial pattern: MEFA has the higher correlation value with RSF3 (the closest station); the correlation values are lower for CAFE and SNAL, slightly higher for the latter.

The horizontal components, the radial and the transverse (see the right side of Figs. 4b and 5b and of Figs. 4c and 5c, respectively), show maximum values of the correlation function that are systematically lower than the vertical ones. For most, the correlation function maximum exceeds the value 0.5 for the earthquakes of 8 January and 26 March. For the earthquake of 12 January, the signal-to-noise ratio is too low to consider the results significant (i.e. the ratio is 5 dB for the radial component of RSF3). The spatial patterns of the cross-correlation of the horizontal components are different. The correlation between MEFA and SNAL is higher for the event of 8 January, while the event of 26 March follows the same spatial distribution of the vertical components, with slightly higher values for the radial components.

Despite the few data analysed, some considerations can be made. The results obtained from the application of the cross-correlation technique show a general likeness between MEFA and RSF3, which are about 3.5 km apart. Due to the small distance and the high correlation values, it is reasonable to assume that the crustal structure below these seismic stations is roughly the same. The low correlation between MEFA-CAFE and MEFA-SNAL could be due to differences between the crustal structure beneath MEFA and that beneath the other two stations. The slightly higher correlation between MEFA and SNAL with respect to MEFA and CAFE suggests that these differences can be more marked in the latter case. In fact, CAFE is located NE of Mt. Forcuso (Frigento) antiform, in the Trevico synform (Fig. 1). The stratigraphic and structural setting of this area is very different from that of the MEFA, RSF3, and SNAL area, as can be deduced by seismic profiles (e.g. Mostardini and Merlini, 1986) and by well stratigraphy [Trevico

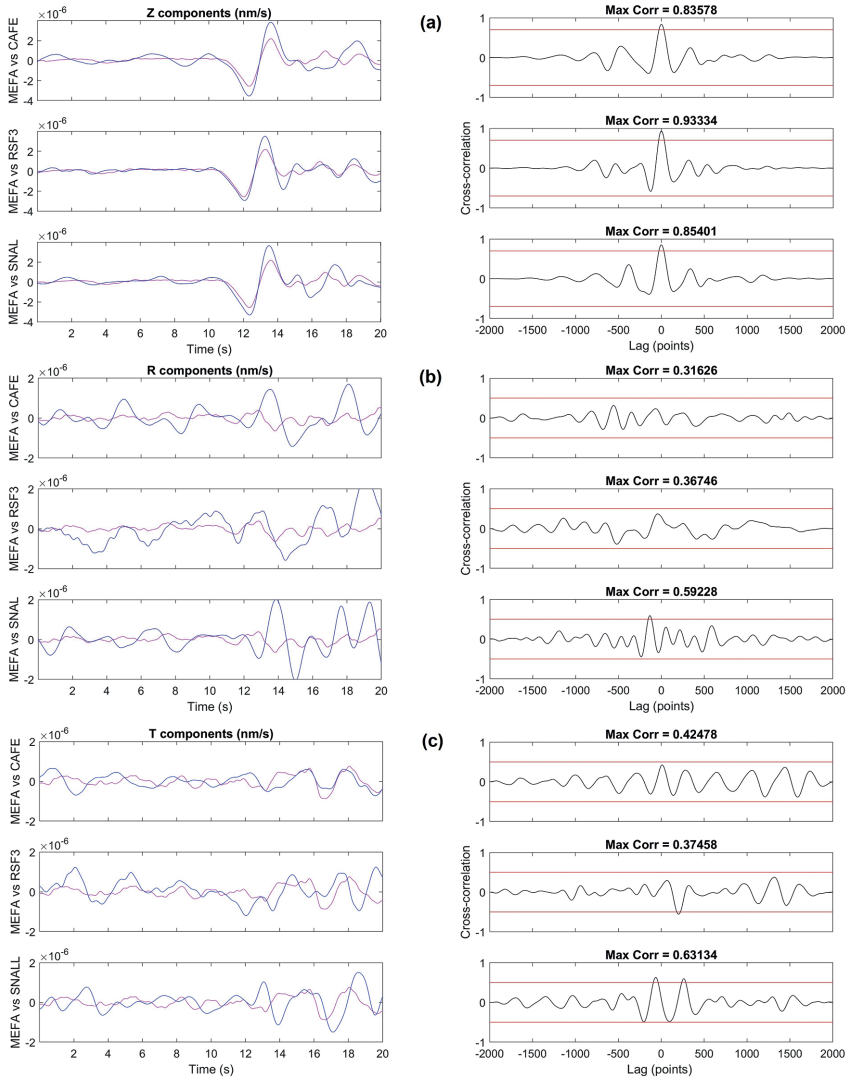

Fig. 4 - Cross-correlation analysis for the teleseismic event of 8 January 2021. Panel a, left side: comparison between the signal of the vertical components of MEFA station (magenta lines) and the other three stations (blue lines); right side: the cross correlations (black lines) as function of lags, expressed in points (100 points = 1 s), relative to the signals shown on the left; the red lines represent the significance level, set at 0.7 for the vertical components. The maximum value of the cross-correlation function is also reported. Panels b and c are the same for the radial and transverse components, respectively. These horizontal components are aligned with respect to the first P arrivals retrieved on the corresponding vertical component. The significance level is set at 0.5 (red lines).

1, Mt. Forcuso 1 and 2 wells (Fig. 1); ViDEPI (2016)].

Looking at the equalised signals shown in Figs. 2 and 3, the general decrease in the direct P-wave amplitude of the waveforms relating to MEFA and RSF3, with respect to the other two seismic stations, is evident. This aspect can be immediately noticed by observing the P-phase amplitude on the vertical components (Fig. 6). The observed decrease is about 40% at MEFA compared to SNAL, the southernmost station, while at RSF3 it is about 15%. The P-phase amplitude at the CAFE and SNAL stations is roughly the same. Looking at the radial components shown in Fig. 6, the amplitudes of MEFA and RSF3 are comparable, whereas the amplitude of

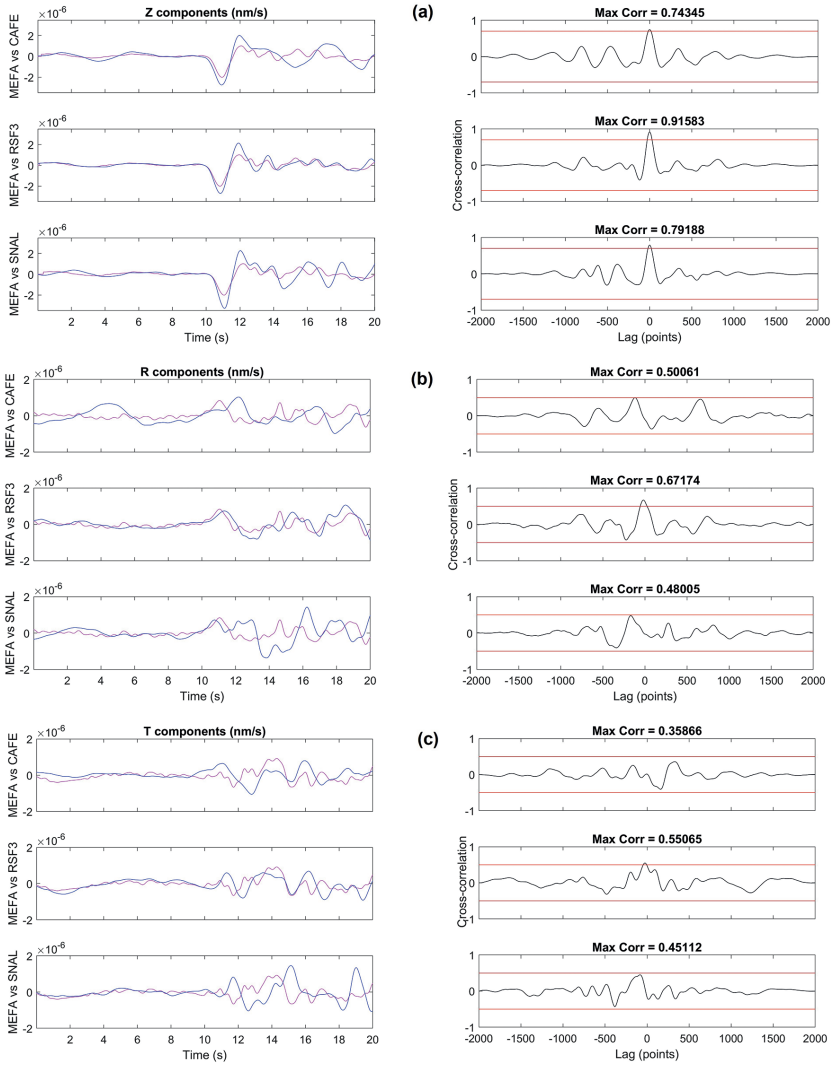

Fig. 5 - Cross-correlation analysis for the teleseismic event of 26 March 2021. Panel a, left side: comparison between the signal of the vertical components of the MEFA station (magenta lines) and the other three stations (blue lines); right side: the cross correlations (black lines) as function of lags, expressed in points (100 points = 1 s), relative to the signals shown on the left; the red lines represent the significance level, set at 0.7 for the vertical components. The maximum value of the cross-correlation function is also reported. Panels b and c are the same for the radial and transverse components, respectively. These horizontal components are aligned with respect to the first P arrivals retrieved on the corresponding vertical component. The significance level is set at 0.5 (red lines).

MEFA with respect to the other two stations is considerably lower. The described amplitude spatial patterns cannot be attributed to site amplification at the two stations that show the higher P-wave amplitudes, SNAL and CAFE, since they are not affected by such effects according to the CRISP project (results available at http://crisp.ingv.it/; last access: December 2022). In this project, the site effects were evaluated with H/V ratio by using background seismic noise, as well as regional earthquakes; both the stations showed H/V curves below level 2, which is considered the threshold for no-significant local amplification.

The decrease in amplitude at MEFA and RSF3 could be due to the presence of a shallow area

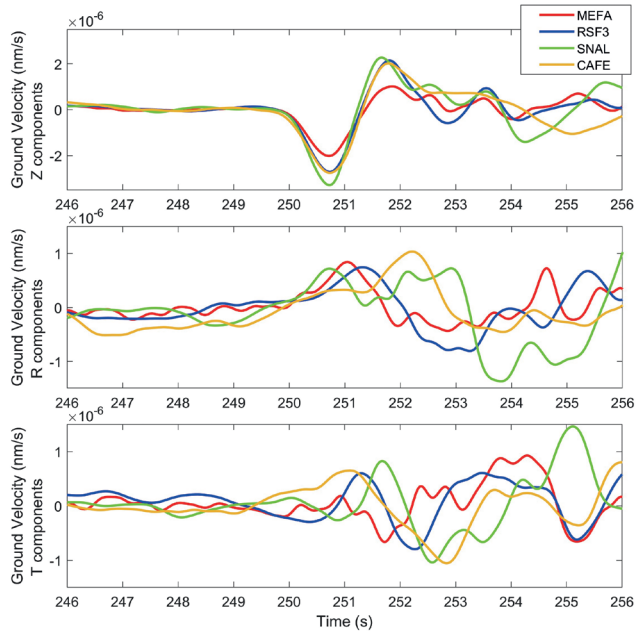

Fig. 6 - Comparison among the waveforms of the teleseismic event of 26 March 2021 and recorded by the stations indicated in the legend (upper-right corner). The ground velocity component is reported in the y-axes labels. The traces are aligned according to the P wave pulse.

beneath these stations characterised by high fluid circulation. The prominence of the crossing of a seismic wave front in an area characterised by strong heterogeneity results in the attenuation of the amplitude of the P and S waves. The presence of a shallow area beneath MEFA and RSF3 characterised by high fluid circulation is in agreement with the models proposed by Improta *et al.* (2014), where a fluid-filled volume of rocks is identified in the area below Mt. Forcuso. The data from the Mt. Forcuso 1 well, about 2 km east of Mefite, fixes a depth of 1128-1600 m for an overpressurised CO_2 gas cap of a deep-seated aqueous reservoir in Apulian fractured limestone, supporting this interpretation.

5. Concluding remarks

We proposed and tested a method to retrieve the teleseismic event waveform similarities by equalising the traces recorded at the seismic stations with different instrumentation. Although the method can be perfected and tested using more teleseismic and regional events, at this stage it allows us to directly compare, in the time domain, the waveforms recorded by several different stations, so as to obtain some information on the crustal structure. Due to the limited time period over which MEFA operated (about 4 months), only few recorded teleseismic events are available and all approach the station from NE. This limitation does not allow the application of certain approaches in modelling the crustal structure based on the best fit between synthetic and observed data. Notwithstanding this, our approach enables obtaining some information about the crustal structure of the explored area, even in a complex geological setting. The comparison between MEFA and RSF3 suggests that the area of diffuse CO_2 degassing is not limited to the emission site but involves a larger area centred on the vents that could extend to a depth of a few kilometres. The comparison between MEFA and the two most distant seismic stations confirms the complexity of the crustal structure in this portion of the Apennine chain.

Acknowledgments. A first excerpt of this paper was presented at the 40th GNGTS meeting held in Trieste on 26-29 June 2022. We are grateful to the two anonymous referees for their critical reviews and useful comments and suggestions on the manuscript. We also thank the editor D. Slejko for the assistance and A. Rebez for the encouragement to submit the paper. The data recorded at Mefite d'Ansanto are subjected to the INGV project's policy. Contact the corresponding author for more information. Data acquired by the other stations are available at https://eida.ingv.it/it/ (free access).

REFERENCES

Amato A., Chiarabba C., Malagnini L. and Selvaggi G.; 1992: *Three-dimensional P-velocity structure in the region of the M_S = 6.9 Irpinia, Italy, normal faulting earthquake*. Phys. Earth Planet. Inter., 75, 111-119, doi: 10.1016/0031-9201(92)90122-C.

Ammon C.; 1991: *The isolation of receiver effects from teleseismic P waveforms*. Bull. Seismol. Soc. Am., 81, 2504-2510.

Amoroso O., Russo G., De Landro G., Zollo A., Garambois S., Mazzoli S., Parente M. and Virieux J.; 2017: *From velocity and attenuation tomography to rock physical modeling: inferences on fluid-driven earthquake processes at the Irpinia fault system in southern Italy*. Geophys. Res. Lett., 44, 6752-6760, doi: 10.1002/2016GL072346.

Ascione A., Ciotoli G., Bigi S., Buscher J., Mazzoli S., Ruggiero L., Sciarra A., Tartarello M.C. and Valente E.; 2018: *Assessing mantle versus crustal sources for non-volcanic degassing along fault zones in the actively extending southern Apennines mountain belt (Italy).* Geol. Soc. Am. Bull., 130, 1697-1722, doi: 10.1130/B31869.1.

Ascione A., Nardò S. and Mazzoli S.; 2020: *The M_S 6.9, 1980 Irpinia Earthquake from the basement to the surface: a review of tectonic geomorphology and geophysical constraints, and new data on postseismic deformation.* Geosci., 10, 493, doi: 10.3390/geosciences10120493.

Castello B., Moschillo R., Pignone M., Vinci S., Doumaz F., Nostro C. and Selvaggi G.; 2008: *Seismicity map of Italy, 2000-2007*. Istituto Nazionale di Geofisica e Vulcanologia-Centro Nazionale Terremoti (INGV-CNT), Roma, Italy.

Chiarabba C. and Amato A.; 1997: *Upper-crustal structure of the Benevento area (southern Italy): fault heterogeneities and potential for large earthquakes.* Geophys. J. Int., 130, 229-239, doi: 10.1111/j.1365-246X.1997.tb01001.x.

Chiodini G., Granieri D., Avino R., Caliro S., Costa A., Minopoli C. and Vilardo G.; 2010: *Non-volcanic CO_2 Earth degassing: case of Mefite d'Ansanto (southern Apennines), Italy.* Geophys. Res. Lett., 37, L11303, doi: 10.1029/2010GL042858.

Clayton R.W. and Wiggins R.A.; 1976: *Source shape estimation and deconvolution of teleseismic bodywaves*. Geophys. J. Int., 47, 151-177.

Cusano P., Del Gaudio P., Galluzzo D., Gaudiosi G., Gervasi A., La Rocca M., Martino C., Milano G., Nardone L., Petrosino S., Torello V., Zuccarello L. and Di Luccio F.; 2021: *Analysis of background seismicity recorded at Mefite d'Ansanto CO_2 emission field in the framework of FURTHER project: first results*. In: Proc. EGU General Assembly, Wien, Austria, EGU21-10625**,** doi: 10.5194/egusphere-egu21-10625.

De Matteo A., Massa B., Milano G. and D'Auria L.; 2018: *A transitional volume beneath the Sannio-Irpinia border region (southern Apennines): different tectonic styles at different depths.* Tectonophys., 723, 14-23.

Di Luccio F., Palano M., Chiodini G., Cucci L., Piromallo C., Sparacino F., Ventura G., Improta L., Cardellini C., Persaud P., Pizzino L., Calderoni G., Castellano C., Cianchini G., Cianetti S., Cinti D., Cusano P., De Gori P., De Santis A., Del Gaudio P., Diaferia G., Esposito A., Galluzzo D., Galvani A., Gasparini A., Gaudiosi G., Gervasi A., Giunchi C., La Rocca M., Milano G., Morabito S., Nardone L., Orlando M., Petrosino S., Piccinini D., Pietrantonio G., Piscini A., Roselli P., Sabbagh D., Sciarra A., Scognamiglio L., Sepe V., Tertulliani A., Tondi R., Valoroso L., Voltattorni N. and Zuccarello L.; 2022: *Geodynamics, geophysical and geochemical observations, and the role of CO_2 degassing in the Apennines*. Earth Sci. Rev., 234, 104236, doi: 10.1016/j.earscirev.2022.104236.

DISS Working Group; 2021: *Database of Individual Seismogenic Sources (DISS), Version 3.3.0: a compilation of potential sources for earthquakes larger than M 5.5 in Italy and surrounding areas.* Istituto Nazionale di Geofisica e Vulcanologia (INGV), Roma, Italy, doi: 10.13127/diss3.3.0.

Frepoli A., Maggi C., Cimini G.B., Marchetti A. and Chiappini M.; 2011: *Seismotectonics of southern Apennines from recent passive seismics experiments.* J. Geodyn., 51, 110-124, doi: 10.1016/j.jog.2010.02.007.

Gibbons S.J. and Ringdal F.; 2006: *The detection of low magnitude seismic events using array-based waveform correlation.* Geophys. J. Int., 165, 149-166, doi: 10.1111/j.1365-246X.2006.02865.x

Harris D. and Paik T.; 2006: *Subspace detectors: efficient implementation*. Lawrence Livermore National Laboratory, Livermore, CA, USA, UCRL-TR-223177, 36 pp. <www.llnl.gov/tid/lof/documents/pdf/336400.pdf>.

Harris D. and Dodge D.; 2011: *An autonomous system for grouping events in a developing aftershock sequence.* Bull. Seismol. Soc. Am., 101, 763-774, doi: 10.1785/0120100103.

Improta L., Bonagura M., Capuano P. and Iannaccone G.; 2003: *An integrated geophysical investigation of the upper crust in the epicentral area of the 1980, Ms = 6.9, Irpinia earthquake (southern Italy)*. Tectonophys., 361, 139-169, doi: 10.1016/S0040-1951(02)00588-7.

Improta L., De Gori P. and Chiarabba C.; 2014: *New insights into crustal structure, Cenozoic magmatism, CO_2 degassing, and seismogenesis in the southern Apennines and Irpinia region from local earthquake tomography.* J. Geophys. Res.: Solid Earth, 119, 8283-8311, doi: 10.1002/2013JB010890.

ISPRA; 2016: *Carta Geologica d'Italia alla scala 1:50.000, foglio 450, S. Angelo dei Lombardi*. <www.isprambiente.gov.it/Media/carg/450_SANTANGELOLOMBARDI/Foglio.html>.

Langston C.A.; 1979: *A single-station fault-plane solution method.* Geophys. Res. Lett., 6, 41-44, doi: 10.1029/GL006i001p00041.

Matano F. and Di Nocera S.; 2001: *Geologia del settore centrale dell'Irpinia (Appennino meridionale): nuovi dati e interpretazioni.* Boll. Soc. Geol. It., 120, 3-14.

Mazzoli S. and Helman M.; 1994: *Neogene patterns of relative plate motion for Africa-Europe: some implications for recent central Mediterranean tectonics*. Geol. Rundsch., 83, 464-468, doi: 10.1007/BF00210558.

Milano G., Bianco F. and Vilardo G.; 2001: *Evidences of P-S conversions beneath the Vesuvius volcanic area (south Italy) from teleseismic data*. Volcanol. Seismol., 5, 73-80.

Milano G., Gervasi A., Morabito S., Cusano P., Del Gaudio P., Galluzzo G., Gaudiosi G., La Rocca M., Nardone L., Petrosino S. and Zuccarello L.; 2022: *First steps towards the upper crustal structure investigation in the area of Mefite d'Ansanto (Italy) by using teleseismic events*. In: Poster 40th Convegno Nazionale, Gruppo Nazionale di Geofisica della Terra Solida (GNGTS), Trieste, Italy, <gngts.ogs.it/archivio/>.

Morabito S., Cusano P., Galluzzo D., Gaudiosi G., Nardone L., Del Gaudio P., Gervasi A., La Rocca M., Milano G., Petrosino S., Zuccarello L., Manzo R., Buonocunto C. and Di Luccio F.; 2023: *One-year seismic survey of the tectonic CO_2-rich site of Mefite d'Ansanto (southern Italy): preliminary insights in the seismic noise wavefield.* Sensors, 23, 1630, doi: 10.3390/s23031630.

Mostardini F. and Merlini S.; 1986: *Appennino centro meridionale: sezioni geologiche e proposta di modello strutturale*. Mem. Soc. Geol. It., 35, 177-202.

Patacca E. and Scandone P.; 1989: *Post-Tortonian mountain building in the Apennines. The role of the passive sinking of a relic lithospheric slab, in the lithosphere in Italy.* In: Proc. The lithosphere in Italy, Advances in Earth Science Research, Boriani A., Bonafede M., Piccardo G.B. and Vai G.B. (eds), Accademia Nazionale dei Lincei, Roma, Italy, Atti del Convegno, 80, 157-176.

Pischiutta M., Anselmi M., Cianfarra P., Rovelli A. and Salvini F.; 2013: *Directional site effects in a non-volcanic gas emission area (Mefite d'Ansanto, southern Italy): evidence of a local transfer fault transversal to large NW-SE extensional faults?* Phys. Chem. Earth Part A/B/C, 63, 116-123, doi: 10.1016/j.pce.2013.03.008.

Roure F., Casero P. and Vially R.; 1991: *Growth processes and mélange formation in the southern Apennines accretionary wedge.* Earth Planet. Sci. Lett., 102, 395-412.

Rovida A., Locati M., Camassi R., Lolli B. and Gasperini P.; 2020: *The Italian earthquake catalogue CPTI15.* Bull. Earthquake Eng., 18, 2953-2984, doi: 10.1007/s10518-020-00818-y.

Rovida A., Locati M., Camassi R., Lolli B., Gasperini P. and Antonucci A. (eds); 2022: *Italian parametric earthquake catalogue (CPTI15), version 4.0*. Istituto Nazionale di Geofisica e Vulcanologia (INGV), Roma, Italy, doi: 10.13127/CPTI/CPTI15.4.

Schaff D.P. and Waldhauser F.; 2005: *Waveform cross-correlation-based differential travel-time measurements at the northern California seismic network*. Bull. Seismol. Soc. Am., 95, 2446-2461.

Schaff D.P. and Waldhauser F.; 2006: *Improving magnitude detection thresholds using multi-station, multi-event, and multi-phase methods.* In: Proc. 28th Seismic Research Review - Ground-Based Nuclear Explosion Monitoring Technologies, Orlando, FL, USA, LA-UR-06-5471, pp. 493-502.

Schaff D.P. and Richards P.G.; 2011: *On finding and using repeating seismic events in and near China.* J. Geophys. Res., 116, B03309, doi: 10.1029/2010JB007895.

Shiner P., Beccacini A. and Mazzoli S.; 2004: *Thin-skinned versus thick-skinned structural models for Apulian carbonate reservoirs: constraints from the Val d'Agri Fields, S Apennines, Italy*. Mar. Pet. Geol., 21, 805-827, doi: 10.1016/j.marpetgeo.2003.11.020.

ViDEPI; 2016: *Progetto ViDEPI - Visibilità dei dati afferenti all'attività di esplorazione petrolifera in Italia* (last upgrade). <www.videpi.com/videpi/pozzi/pozzi.asp>.

Corresponding author: Girolamo Milano
Istituto Nazionale di Geofisica e Vulcanologia, Sezione di Napoli – Osservatorio Vesuviano
Via Diocleziano 328, 80124 Napoli, Italy
Phone: +39 081 6108331, e-mail: girolamo.milano@ingv.it